

# Novel template-free synthesis of hollow@porous TiO<sub>2</sub> superior anode materials for lithium ion battery

Peigen Zhang<sup>1</sup> · Chunyan Zhang<sup>1</sup> · Anjian Xie<sup>1</sup> · Cun Li<sup>1</sup> · Jiming Song<sup>1</sup> · Yuhua Shen<sup>1</sup>

Received: 17 October 2015 / Accepted: 10 December 2015 / Published online: 21 December 2015  
© Springer Science+Business Media New York 2015

**Abstract** Template-free method is used to facilely synthesize TiO<sub>2</sub> hollow microspheres via one-step hydrothermal method. Interestingly, the TiO<sub>2</sub> hollow microspheres have porous shell with thickness of about 450 nm. The formation mechanism of the hollow@porous TiO<sub>2</sub> microspheres involves the formation and aggregation of TiO<sub>2</sub> nanoparticles followed by oriented growth, etching of HF, and then Ostwald ripening and transformation process. The prepared TiO<sub>2</sub> microspheres show a reversible capacity of ~170 mAh g<sup>-1</sup> after 150 cycles at a current density of 0.6 C and also exhibit a good rate capability of 40.8 mAh g<sup>-1</sup> at a current density of 24 C due to the unique hollow@porous structure, which can offer more sites for the storage and insertion of Li ions, and accelerate electrolyte diffusion and Li ions transport. The results also indicate that the as-prepared TiO<sub>2</sub> material possesses excellent electrochemical performances, which may be an ideal anode material for lithium ion battery.

## Introduction

Low-cost and convenient synthesis has been considered as a promising method; researchers are devoted themselves to explore how to reduce the work and make the cost lower in

different fields. As we know, the hollow structure materials have raised interest in various fields such as photocatalysis, drug delivery, and others due to the advantages of high surface area, good adsorption, and low density. Researchers also have controllably synthesized hollow structure by diverse strategies. Among these methods, the hard and soft template methods are popularly used. The hard templates, such as carbon spheres, carbon nanotubes, silica, and some easy to be removed materials, are served as the sacrificial templates to prepare hollow structure by two-step methods, but they are high cost and troublesome. The soft template method, using ethylene glycol, polyvinylpyrrolidone, and sodium dodecyl benzene sulfonate as inducers, is a convenient method for synthesizing hollow structure, but the post-processing is difficult and the cost is increased [1, 2]. So it is obvious that a facile method with low cost to synthesize hollow structure materials massively is important and necessary.

Titanium dioxide (TiO<sub>2</sub>) is considered as a promising anode material because of the advantages of low cost, safety, non-toxic, structural stability, and high voltage plateau, and has attracted extensive attention. Some researchers fabricated graphene/TiO<sub>2</sub> hybrid materials, carbon-tube/TiO<sub>2</sub> composite, and TiO<sub>2</sub>@carbon to improve the electrochemical performance [3–5]. But many researchers still tend to study the hollow TiO<sub>2</sub> materials because the hollow structures can make Li ions access the shells of the spheres from both sides, shorten the diffusion path and improve kinetics, leading to good cycle performance, high rate capacity, and excellent lithium storage. In addition, the hollow structure can buffer structural strain caused during Li ions insertion and expulsion, improving the structural stability and cycling life. Wang and Lou [6] prepared TiO<sub>2</sub> nanocages by employing Cu<sub>2</sub>O polyhedra as the hard template to improve the reversible capacity and

**Electronic supplementary material** The online version of this article (doi:10.1007/s10853-015-9662-0) contains supplementary material, which is available to authorized users.

✉ Yuhua Shen  
s\_yuhua@163.com; yuhuashen@ahu.edu.cn

<sup>1</sup> School of Chemistry and Chemical Engineering, Lab for Clean Energy & Green Catalysis, Anhui University, Hefei 230601, People's Republic of China

cycling performance. Xiao et al. [7] synthesized the uniform and monodispersed TiO<sub>2</sub> hollow spheres by utilizing carboxyl-functionalized polystyrene spheres as hard templates, improving the discharge–charge capacity due to the facility and reversibility of lithium storage on surface. Zhang et al. [8] fabricated anatase TiO<sub>2</sub> hollow spheres with high crystallinity by employing the carbon as template, which shows the excellent property of lithium storage. Ren et al. [9] obtained the uniform multishelled TiO<sub>2</sub> hollow microspheres via sacrificing hard template to control the shell thickness and the number of internal shells. The above studies on fabricating hollow structure using template methods are troublesome and the cost is high. So to fabricate TiO<sub>2</sub> hollow structure by the template-free method will be more convenient and lower cost, which is easy for the large-scale production. Therefore, the template-free method for the preparation of the hollow TiO<sub>2</sub> is worthy to be explored.

Herein, we report a simple synthesis for hollow as well as porous TiO<sub>2</sub> microspheres via one-step hydrothermal method without template. The formation and growth mechanism of these TiO<sub>2</sub> microspheres have been explored by the intermediate products obtained at different reaction stages. Meanwhile, the hollow structure exhibits high reversible capacity, excellent rate capability, and cycling stability as the anode material and may have a good prospect for LIBs.

## Experimental

### Materials

Titanium tetrachloride (TiCl<sub>4</sub>, 99.0 %) and ammonium hexafluorotitanate (IV) ((NH<sub>4</sub>)<sub>2</sub>TiF<sub>6</sub>, 98.0 %) were purchased from Aladdin industrial Corporation (P. R. China). All reagents were of analytical grade and were employed without further purification. Milli-Q water (Millipore Corp., with resistivity of 18.2 MΩ cm) was used for the experiments.

### Synthesis of hollow@porous TiO<sub>2</sub> microspheres

Hollow@porous TiO<sub>2</sub> microspheres were synthesized via one-step hydrothermal method. Firstly, (NH<sub>4</sub>)<sub>2</sub>TiF<sub>6</sub> solution (0.1 mol L<sup>-1</sup>, 10 mL) was poured into the TiCl<sub>4</sub> solution (0.1 mol L<sup>-1</sup>, 10 mL) under magnetic stirring for 5 min. Then, the mixture was transferred into a Teflon-lined stainless autoclave and heated at 150 °C for 10 h. After cooling to room temperature, the product was collected by centrifugation, rinsed with Milli-Q water for several times, and dried at 80 °C for 10 h. The weight of obtained product is 0.1120 g.

The time-dependent experiments for hydrothermal time of 10 min, 1, and 6 h were also performed under the same conditions.

### Characterization

The X-ray diffraction (XRD) patterns were performed on DX-2700 (Dandong Haoyuan instrument Co., Ltd., P. R. China) using Cu-Kα ( $\lambda = 1.5406 \text{ \AA}$ ) radiation, and the accelerating voltage and applied current were 35 kV and 25 mA. Field emission scanning electron microscopy (FESEM) images were taken with a Hitachi S4800 scanning electron microscope. Transmission electron microscopy (TEM) measurements were carried out on JEM model 100SX electron microscopes (Japan Electron Co., Ltd.) operated at an accelerating voltage of 200 kV. Energy dispersive spectra were analyzed on INCA x-act energy dispersive spectrometer with a voltage 15 kV (Oxford Instruments).

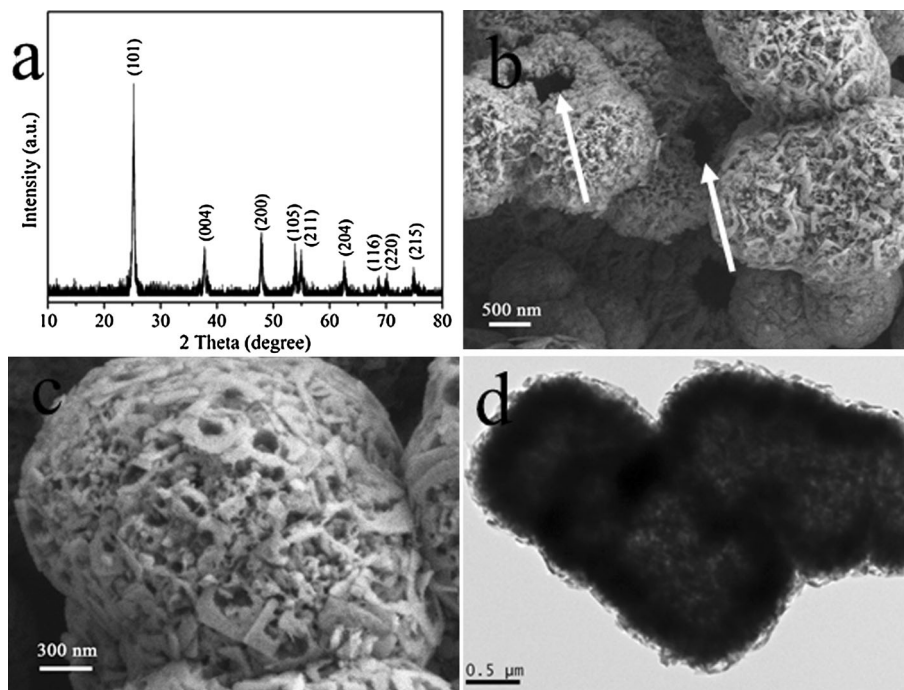
### Electrochemical measurement

The working electrodes were composed of active material, acetylene black, and polyvinylidene fluoride (PVDF) in a weight ratio of 70:20:10. The mass loading of active material for each circular electrode ( $d = 14 \text{ mm}$ ) is about 2.2 mg (1.43 mg cm<sup>-2</sup>). Copper foil, metallic lithium, and polyethylene film (Celgard, 2400) were employed as the collector, counter electrode, and separator, respectively. LiPF<sub>6</sub> (1 M) in the mixed solution of ethylene carbonate (EC) and dimethyl carbonate (DMC) (1:1 in volume ratio) was used as the electrolyte. The coin cells (CR2032) were assembled in an argon-filled glove box. The galvanostatic charge and discharge were performed on a battery testing system (CT-3008W-5V 10 mA, Neware Technology Co., Ltd., P. R. China) at various current densities between 1.0 and 3.0 V (vs. Li<sup>+</sup>/Li). Cyclic voltammetry (CV) measurement was carried out on an electrochemical workstation (CHI660D, Shanghai CH instruments Co., Ltd. P. R. China) between 1.0 and 3.0 V (vs. Li<sup>+</sup>/Li) at a scanning rate of 0.1 mV s<sup>-1</sup>. The voltage selection of above experiments was according to the references [8, 10–12]. Electrochemical impedance spectroscopy (EIS) was measured on the electrochemical workstation with the frequency from 100 kHz to 0.01 Hz.

### Results and discussion

Figure 1a represents the XRD patterns of the TiO<sub>2</sub> synthesized at hydrothermal reaction time of 10 h. The nine diffraction peaks at  $2\theta$  of 25.28°, 37.80°, 48.05°, 53.89°, 55.06°, 62.69°, 68.76°, 70.31°, and 75.03° can be indexed as the anatase TiO<sub>2</sub> for the lattice plane of (101), (004),

**Fig. 1** **a** XRD pattern, **b**, **c** SEM, and **d** TEM images of hollow@porous TiO<sub>2</sub> microspheres fabricated at hydrothermal reaction time of 10 h



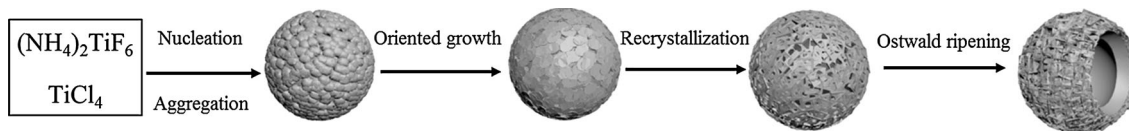
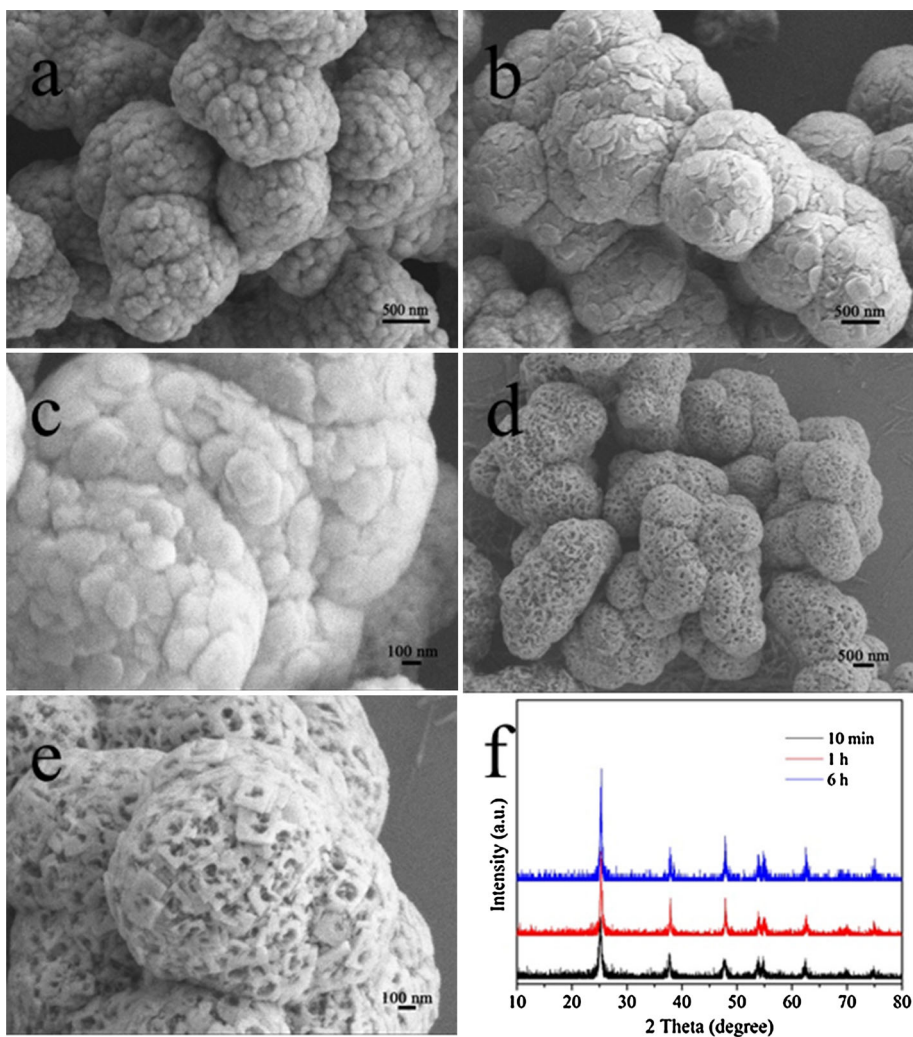
(200), (105), (211), (204), (116), (220), and (215), which is consistent with the standard card (JCPDS NO. 21-1272). The sharp diffraction peaks indicate the good crystallization of the as-prepared TiO<sub>2</sub>. The TiO<sub>2</sub> sample is also confirmed as a high purity because there is no diffraction peaks of other impurity phase as shown in Fig. 1a. Meanwhile, we can find that only the peaks of titanium and oxygen elements are detected in the EDS spectrum hollow@porous TiO<sub>2</sub> microspheres (Fig. S1). The atomic ratio of the two elements is 1: 2.11, which is closed to the composition of TiO<sub>2</sub>. The result further proves that the sample is pure. Figure 1b, c exhibits SEM images of TiO<sub>2</sub> sample obtained at hydrothermal time of 10 h. The TiO<sub>2</sub> microspheres with porous surfaces composed of nanosheets are clearly discovered. From the broken part of the sphere in Fig. 1b, we find that the TiO<sub>2</sub> microspheres are hollow, which is confirmed by the TEM images (Fig. 1d) of TiO<sub>2</sub> microspheres. The contrast of uneven darker edges and pale centers further prove the TiO<sub>2</sub> microspheres are with hollow structure and porous surface. The shell thickness of hollow@porous TiO<sub>2</sub> microspheres is about 450 nm.

Figure 2 shows time-dependent SEM images of TiO<sub>2</sub> samples. The TiO<sub>2</sub> microspheres with rough surfaces are assembled by many TiO<sub>2</sub> nanoparticles with average diameter of 140 nm, which can be detected in Fig. 2a at hydrothermal time of 10 min. When the reaction time reaches 1 h, the nanoparticles changed to nanoplates with a thickness of about 10 nm, as shown in Fig. 2b, c. As the reaction time prolonged to 6 h, many holes are observed on the nanoplates and make the surface of the TiO<sub>2</sub>

microspheres very rough (Fig. 2d, e). When the hydrothermal time is 10 h, the nanoplates with holes disappear, and then the rough surface of TiO<sub>2</sub> microspheres with pores is seen in Fig. 1b, c. We can also detect that the peak intensity at  $2\theta$  of 25.28° in Fig. 2f and Fig. 1a increases clearly with the time extension, indicating the oriented growth of (101) crystal plane.

The probable formation mechanism of hollow TiO<sub>2</sub> microspheres with porous shell is illustrated in Fig. 3. When TiCl<sub>4</sub> is added into water, Ti-OH groups are generated due to the hydrolysis of TiCl<sub>4</sub> and accompanied by the generation of a large amount of hydrochloric acid (HCl). In the initial of the hydrothermal reaction, Ti-F groups of (NH<sub>4</sub>)TiF<sub>6</sub> can easily combine with Ti-OH groups to form Ti-O-Ti oxygen bridge bonds by releasing hydrofluoric acid (HF) [13], resulting in the formation of TiO<sub>2</sub> nanoparticles followed by their aggregation to form TiO<sub>2</sub> microspheres (Fig. 2a). With the reaction time extended, the surface energy of the (001) crystal plane can be reduced to a lower level than that of (101) crystal plane due to the adsorption of F<sup>-</sup> on the (001) crystal plane, resulting in the oriented growth of (101) crystal plane and the exposure of (001) crystal plane [14, 15], then the nanoplates will appear (Fig. 2b, c). As the reaction continued, HF generated at the initial stage of hydrothermal reaction etches the (001) crystal plane and the etching started from the central area of the TiO<sub>2</sub> nanoplates due to the higher density of planar defects [14], resulting in the formation of TiO<sub>2</sub> microspheres with rough surface (Fig. 2d, e). Ostwald ripening can be employed to explain

**Fig. 2** SEM images of TiO<sub>2</sub> microspheres obtained at hydrothermal reaction time of **a** 10 min, **b**, **c** 1 h, and **d**, **e** 6 h, **f** XRD patterns of the TiO<sub>2</sub> samples synthesized at different reaction times



**Fig. 3** Schematic illustration of the probable formation mechanism of hollow@porous TiO<sub>2</sub> microspheres

the formation of hollow microspheres with porous shell [15, 16]. The interiors of TiO<sub>2</sub> microspheres with relative low crystallinity are gradually dissolved by HF shown in Eq. (1), then transferred to the external surface, and recrystallized on the shell of the TiO<sub>2</sub> microspheres indicated by Eq. (2) [17].

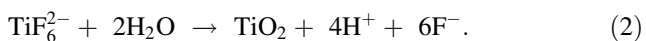
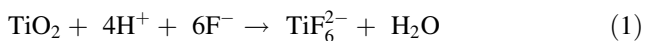
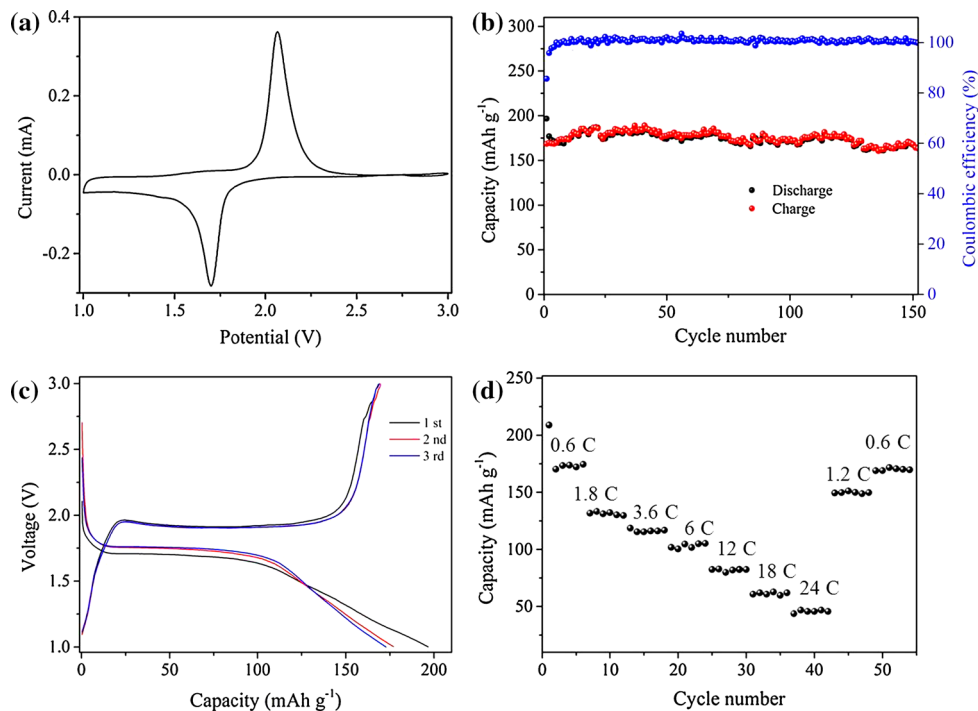


Figure 4a shows the cyclic voltammogram (CV) of hollow@porous TiO<sub>2</sub> microsphere electrode at a scan rate of 0.1 mV s<sup>-1</sup>. A pair of oxidation and reduction peaks can

be noticed at 2.066 V (anodic sweep) and 1.699 V (cathodic sweep), corresponding to extraction and insertion of lithium ion in TiO<sub>2</sub>. The initial three charge–discharge curves of TiO<sub>2</sub> hollow microsphere electrode at a current density of 0.6 C are exhibited in Fig. 4b. Two voltage plateaus appear at ~1.7 and ~2.0 V during the discharge and charge processes, which are consistent with the above CV analysis as well as the previous reports [9, 18]. The first discharge capacity is 196.6 mAh g<sup>-1</sup> and the following charge capacity is 168.4 mAh g<sup>-1</sup>, leading to a capacity loss of 14.4 %. The irreversible capacity loss is attributed to the trapping of lithium ion in TiO<sub>2</sub> nanostructure.



**Fig. 4** Electrochemical performances of hollow@porous TiO<sub>2</sub> microsphere electrode: **a** cyclic voltammogram at a scan rate of 0.1 mV s<sup>-1</sup>; **b** charge–discharge profiles for the initial cycles; **c** cycle performance and coulombic efficiency at 0.6 C (1C = 168 mA g<sup>-1</sup>); **d** Rate capability at various current densities



Furthermore, the subsequent cycles are almost the same, which is also shown in Fig. 4c. The discharge and charge capacities of hollow@porous TiO<sub>2</sub> microspheres are 167.4 and 167.9 mAh g<sup>-1</sup> at a current density of 0.6 C after 150 cycles, respectively. The coulombic efficiency is nearly 100 % at the cycles. The rate capability of the hollow@porous TiO<sub>2</sub> microsphere electrode is estimated by the discharge and charge at various current densities from 0.6 to 24 C as shown in Fig. 4d. When the current density is 0.1 A g<sup>-1</sup>, the capacity is 172.2 mAh g<sup>-1</sup>, and the capacity is still retained in 40.8 mAh g<sup>-1</sup> at high current density of 24 C. After the discharge–charge cycles at high current densities, the capacity of 170.6 mAh g<sup>-1</sup> can be regained when the current density is reduced to 0.6 C, indicating the good rate capability and the stable structure of TiO<sub>2</sub> hollow microspheres.

The good electrochemical performance of hollow@porous TiO<sub>2</sub> microspheres as anode materials for LIBs can be considered from two viewpoints. First, the porous shell of TiO<sub>2</sub> hollow microspheres makes the electrolyte more easily immersed into the interiors of TiO<sub>2</sub> microspheres. The electrolyte is closely contact with the active materials, which shortens the diffusion distance of lithium ion in the discharge–charge processes, promoting the reversible and fast lithium extraction and insertion. Second, the hollow structure can prevent the aggregation of active materials, which maintains the integrity of electrode and prolongs cycle numbers.

Electrochemical impedance spectroscopy (EIS) is further utilized to analyze electrochemical impedance of TiO<sub>2</sub> hollow microsphere electrode. The Nyquist plots of the hollow TiO<sub>2</sub> microsphere electrode before and after cycles are shown in Fig. 5, which display a semicircle in the high-frequency region and an inclined line in the low-frequency range, respectively, corresponding to the charge transfer resistance on the electrode and electrolyte interface and the solid-state diffusion of lithium ion in the electrode materials. The intercept at the real axis in high frequency is related to the electrolyte resistance [19]. The charge

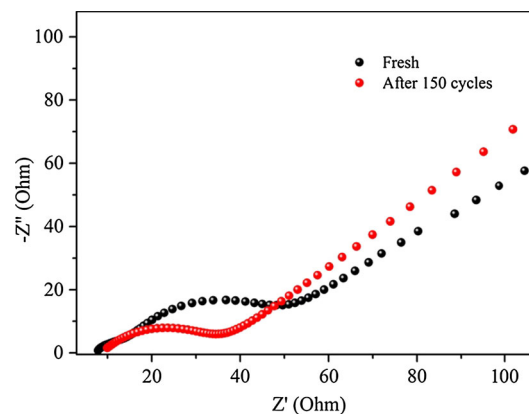


**Fig. 5** Electrochemical impedance spectra of hollow@porous TiO<sub>2</sub> microsphere electrode before and after cycles

transfer is reduced as evidenced by smaller diameter of the semicircle in Nyquist plot of EIS after 150 cycles. The possible reason is likely related to better wetting of the electrolyte to hollow@porous TiO<sub>2</sub> active materials, making more sufficient contact between the active materials and the electrolyte, and then lithium ions and electron can be transferred effectively in the interface of active materials and electrolyte [20, 21]. This results in the enhanced hollow@porous TiO<sub>2</sub> microsphere electrode reaction kinetics and the better cycling performance. In theory, the angle of the inclined line is absolutely 45°, but it is rare in the real cases. Here, the deviation of the 45° line is likely caused by convolution between Warburg diffusion and the capacitance between the two current collectors [22].

## Conclusion

The hollow@porous TiO<sub>2</sub> microspheres are successfully synthesized by a facile hydrothermal method without template. The hollow@porous TiO<sub>2</sub> microsphere electrode keeps a reversible capacity of ~170 mAh g<sup>-1</sup> at a current density of 0.6 C for 150 cycles. Meanwhile, the electrode exhibits a good rate capability, which is evaluated by the discharge–charge cycles at various current densities. The hollow@porous structure of TiO<sub>2</sub> microspheres is beneficial to enhance the electrochemical performances. These hollow@porous TiO<sub>2</sub> microspheres will be a promising material applied in LIBs or other areas.

**Acknowledgements** This work was supported by the National Nature Science Foundation of China (21173001 and 21371003).

## References

1. Wang HE, Jin J, Cai Y et al (2014) Facile and fast synthesis of porous TiO<sub>2</sub> spheres for use in lithium ion batteries. *J Colloid Interface Sci* 417:144–151
2. Zhang P, Zhang J, Xie A, Li S, Song J, Shen Y (2015) Hierarchical flower-like Bi<sub>2</sub>WO<sub>6</sub> hollow microspheres: facile synthesis and excellent catalytic performance. *RSC Adv* 5:23080–23085
3. Yan Z, Liu L, Guo H et al (2014) One-pot synthesis of FCNTs-wired TiO<sub>2</sub> nanocomposites as anode materials for high-rate lithium ion batteries. *Electrochim Acta* 123:551–559
4. Trang NT, Ali Z, Kang DJ (2015) Mesoporous TiO<sub>2</sub> spheres interconnected by multiwalled carbon nanotubes as an anode for high-performance lithium ion batteries. *ACS Appl Mater Interfaces* 7:3676–3683
5. Zhao C, Liu L, Zhang Q, Rogers J, Zhao H, Li Y (2015) Synthesis of carbon-TiO<sub>2</sub> nanocomposites with enhanced reversible capacity and cyclic performance as anodes for lithium-ion batteries. *Electrochim Acta* 155:288–296
6. Wang Z, Lou XW (2012) TiO<sub>2</sub> nanocages: fast synthesis, interior functionalization and improved lithium storage properties. *Adv Mater* 24:4124–4129
7. Xiao L, Cao M, Mei D et al (2013) Preparation and electrochemical lithium storage features of TiO<sub>2</sub> hollow spheres. *J Power Sources* 238:197–202
8. Zhang G, Wu HB, Song T, Paik U, Lou XW (2014) TiO<sub>2</sub> hollow spheres composed of highly crystalline nanocrystals exhibit superior lithium storage properties. *Angew Chem* 53:12590–12593
9. Ren H, Yu R, Wang J et al (2014) Multishelled TiO<sub>2</sub> hollow microspheres as anodes with superior reversible capacity for lithium ion batteries. *Nano Lett* 14:6679–6684
10. Yi J, Lu D, Li X, Hu S, Li W, Lei J, Wang Y (2011) Preparation and performance of porous titania with a trimodal pore system as anode of lithium ion battery. *J Solid State Electrochem* 16:443–448
11. Xia T, Zhang W, Murowchick J, Liu G, Chen X (2013) Built-in electric field-assisted surface-amorphized nanocrystals for high-rate lithium-ion battery. *Nano Lett* 13:5289–5296
12. Madej E, Ventosa E, Klink S, Schuhmann W, La Mantia F (2014) Aging effects of anatase TiO<sub>2</sub> nanoparticles in Li-ion batteries. *Phys Chemistry Chem Phys* 16:7939–7945
13. Yu J, Zhang J (2010) A simple template-free approach to TiO<sub>2</sub> hollow spheres with enhanced photocatalytic activity. *Dalton Trans* 39:5860–5867
14. Shi Q, Li Y, Zhan E, Ta N, Shen W (2014) Anatase TiO<sub>2</sub> hollow nanosheets: dual roles of F<sup>-</sup>, formation mechanism and thermal stability. *CrystEngComm* 16:3431–3437
15. Lv K, Cheng B, Yu J, Liu G (2012) Fluorine ions-mediated morphology control of anatase TiO<sub>2</sub> with enhanced photocatalytic activity. *Phys Chem Chem Phys* 14:5349–5362
16. Yang HG, Zeng HC (2004) Preparation of hollow anatase TiO<sub>2</sub> nanospheres via Ostwald ripening. *J Phys Chem B* 108:3492–3495
17. Yu J, Xiang Q, Ran J, Mann S (2010) One-step hydrothermal fabrication and photocatalytic activity of surface-fluorinated TiO<sub>2</sub> hollow microspheres and tabular anatase single micro-crystals with high-energy facets. *CrystEngComm* 12:872–879
18. Wang X, Wang Y, Yang L, Wang K, Lou X, Cai B (2014) Template-free synthesis of homogeneous yolk–shell TiO<sub>2</sub> hierarchical microspheres for high performance lithium ion batteries. *J Power Sources* 262:72–78
19. Wang S, Xing Y, Su H, Zhang S (2014) MnO nanoparticles interdispersed in 3D porous carbon framework for high performance lithium-ion batteries. *ACS Appl Mater Interfaces* 6:12713–12718
20. Jadhav HS, Kalubarme RS, Park CN, Kim J, Park CJ (2014) Facile and cost effective synthesis of mesoporous spinel NiCo<sub>2</sub>O<sub>4</sub> as an anode for high lithium storage capacity. *Nanoscale* 6:10071–10076
21. Wu F, Huang R, Mu D, Wu B, Chen S (2014) New synthesis of a foamlike Fe<sub>3</sub>O<sub>4</sub>/C composite via a self-expanding process and its electrochemical performance as anode material for lithium-ion batteries. *ACS Appl Mater Interfaces* 6:19254–19264
22. Wen CJ, Ho C, Boukamp BA, Raistrick ID, Weppner W, Huggins RA (1981) Use of electrochemical methods to determine chemical-diffusion coefficients in alloys: application to ‘LiAl’. *Int Metals Rev* 5:253–268